Strain-dependent activation energy of shear transformation in metallic glasses

Bin Xu, Michael Falk, Jinfu Li, and Lingti Kong

Strain-dependent activation energy of shear transformation in metallic glasses

Bin Xu,[1] Michael Falk,[2, *] Jinfu Li,[1] and Lingti Kong[1, †]

[1]*School of Materials Science & Engineering,*

Shanghai Jiao Tong University, Shanghai 200240, China

[2]*Department of Materials Science & Engineering,*

and Department of Mechanical Engineering and the Department of Physics and Astronomy,

Johns Hopkins University, Baltimore, MD 21218, USA

(Dated: March 21, 2017)

Abstract

Shear transformation (ST) plays a decisive role in determining the mechanical behavior of metallic glasses, which is believed to be a stress-assisted thermally activated process. Understanding the dependence in its activation energy on the stress imposed on the material is of central importance to model the deformation process of metallic glasses and other amorphous solids. Here a theoretical model is proposed to predict the variation of the minimum energy path (MEP) associated with a particular ST event upon further deformation. Verification based on atomistic simulations and calculations are also conducted. The proposed model reproduces the MEP and activation energy of an ST event under different imposed macroscopic strains based on a known MEP at a reference strain. Moreover, an analytical approach is proposed based on the atomistic calculations, which works well when the stress varies linearity along the MEP. These findings provide necessary background for understanding the activation processes and, in turn, the mechanical behavior of metallic glasses.

* mfalk@jhu.edu

† konglt@sjtu.edu.cn

I. INTRODUCTION

Metallic glasses, which exhibit unique mechanical properties, have attracted substantial research efforts since their discovery in 1959 [1]. Nonetheless many mysteries still remain to be uncovered. One such mystery relates to the mechanical behavior of metallic glasses: the lack of dislocation-like defects in the amorphous structure makes it difficult to characterize their plastic deformation mechanism. In this regard, many theoretical models [2–9] have been developed to describe the dominant deformation mechanism. One of the key issues in these models is the stress or strain dependence of the activation energies for the shear transformation (ST) events (also sometimes referred to as inelastic events, flow defects, and local inelastic transformations). The Erying model [10], which assumes a linear dependence of the activation energy on the macroscopic stress, has been widely used in the development of theories and the application of kinetic Monte Carlo simulations to study the mechanical behavior of metallic glasses [4, 11–13]. This linear dependence is appropriate when describing the variation of activation energy upon small stress changes, since it is equivalent to considering only the first term in the Taylor expansion of the activation energy with respect to the macroscopic stress. When the stress changes are large, however a nonlinear dependence is often observed in simulations [14–16]. To describe such nonlinear behavior, the catastrophe theory was proposed that predicts a scaling law of $Q \sim (\sigma_c - \sigma)^{\frac{3}{2}}$ (here Q is the activation energy, σ_c is the critical stress at which Q vanishes, and σ is the stress applied) [14]. The accuracy of the catastrophe theory in describing the variation of the activation energy depends on whether the simple Taylor expansion of the energy with respect to the reaction coordinate and the macroscopic stress adequately captures the intrinsic physics of the complex energy landscape, especially far away from the critical stress such that errors introduced by neglecting the high-order Taylor expansion terms become nontrivial. It is also noticed that in order to estimate the stress dependent activation energy based on the catastrophe theory, one needs to know the critical stress *a prior* as well as other characteristics of the energy landscape which make it impractical to predict the activation energy at arbitrary strain before an event is triggered. As such, the intrinsic mechanism governing the influence of stress on the activation energy change is still not clear. To resolve this issue, we re-examine this problem by analyzing how macroscopic strain changes the local energy landscape, i.e., the minimum energy path (MEP) associated with a particular ST event subjected to dif-

2

ferent macroscopic strains. A theoretical model without any fitting parameters is proposed to describe the macroscopic strain dependence of the activation energy of a local ST event based on its known MEP at a referential macroscopic strain level. This methodology is seen to work reasonably well in predicting the macroscopic strain dependence of the activation energies of local ST events identified in a Cu-Zr metallic glass.

This paper is organized as follows. First, the theoretical model which describes the variation of an activation energy against macroscopic strains is described, followed by the computational methods employed and the simulation details adopted to verify the proposed theoretical model. Then, a simplified analytical approach is also proposed based on two assumptions inspired by the simulation results. In the final section we draw some general conclusions.

II. THEORY

Exploring the energy landscape has been an indispensable way to understand the mechanical behavior of metallic glasses [17–22]. We will examine here how macroscopic strains (stresses) affect one dimension of the complex energy landscape, i.e. the MEP of a particular ST event. By evaluating the energy difference between the corresponding configurations along the MEPs at different imposed macroscopic strains, we will be able to quantify the macroscopic strain dependence on the activation energy of the ST event.

To simplify the presentation we only consider simple shear, although all the results to follow are easily generalizable. The reader can easily extend it to other complex deformation modes. Suppose the MEP of an ST event at a macroscopic strain level of γ_0 is known as $E(x, \gamma_0)$, where x is the reaction coordinate that corresponds to a configuration along the MEP. Its counterpart along the MEP at another macroscopic strain level of γ, can be acquired by a macroscopic deformation from γ_0 to γ, with a dominating affine displacement field and a non-affine one [23] which is uncorrelated with the current ST event due to the fixed reaction coordinate. Consequently, the energy difference between them could be estimated as

$$E(x, \gamma) - E(x, \gamma_0) = \Delta E_{\mathrm{af}}(x, \gamma) + \Delta E_{\mathrm{naf}}(\gamma), \tag{1}$$

where $\Delta E_{\mathrm{af}}(x, \gamma)$ is the energy difference between them due to the affine displacement, and $\Delta E_{\mathrm{naf}}(\gamma)$ is the contribution from structural relaxations other than the current event. In

the vicinity of the current ST event (the shear transformation zone, STZ) we assume that no other ST events are expected to be triggered within the strain range under consideration, as those events may lead to significant changes in the MEP. The former term, which depends on x, can be approximated as

$$\Delta E_{\text{af}}(x,\gamma) = \int_{\gamma_0}^{\gamma} V \cdot \tau_{\text{af}}(x,\gamma')\mathrm{d}\gamma', \tag{2}$$

where V is the volume of the system and $\tau_{\text{af}}(x,\gamma')$ is the macroscopic shear stress due to affine displacement for the configuration with a reaction coordinate of x at the macroscopic strain level of γ'. Consequently, the MEP at γ can be estimated as

$$E(x,\gamma) = E(x,\gamma_0) + \int_{\gamma_0}^{\gamma} V \cdot \tau_{\text{af}}(x,\gamma')\mathrm{d}\gamma' + \Delta E_{\text{naf}}(\gamma). \tag{3}$$

The macroscopic stress τ_{af} depends on both x and γ, which will dominate the change in the shape of the MEP. That is to say, it is the difference in the elastic energy changes of the configurations along the MEP upon further deformation that leads to the MEP variation, and in turn the variation in the activation energy. It should be noted that although the configurations along the MEP at γ_0 lie in a valley of the energy landscape, there is a chance that upon further deformation to γ configurations along a neighboring path might present an alternate and more favorable MEP. In this instance it would be impossible to locate the counterpart of a configuration at γ_0 by an affine deformation. Nonetheless, the new MEP generally has a lower activation energy than that along the affinely-deformed one, and the above estimation still serves as an upper limit. We will show that the error in predicting the activation energy change introduced by such migration effect can be ignored in most, if not all, of the ST events.

The stress difference between $\tau_{\text{af}}(x,\gamma)$ and $\tau(x,\gamma_0)$, however depends marginally on x while mainly on γ, since variation in x corresponds to local structural adjustments which do not greatly affect the affine deformation modulus [23, 24]. Thus, we have

$$\tau_{\text{af}}(x,\gamma) - \tau(x,\gamma_0) = f(\gamma). \tag{4}$$

As a result, the MEP at γ given by Eq. 3 will be

$$E(x, \gamma) = E(x, \gamma_0) + V \int_{\gamma_0}^{\gamma} [\tau(x, \gamma_0) + f(\gamma')]\mathrm{d}\gamma' + \Delta E_{\mathrm{naf}}(\gamma), \tag{5}$$

$$= E(x, \gamma_0) + V \cdot \tau(x, \gamma_0) \cdot (\gamma - \gamma_0) + V \int_{\gamma_0}^{\gamma} f(\gamma')\mathrm{d}\gamma' + \Delta E_{\mathrm{naf}}(\gamma),$$

$$= E(x, \gamma_0) + V \cdot \Delta\tau(x, \gamma_0) \cdot (\gamma - \gamma_0) + V \cdot \tau(x_{m,\gamma_0}, \gamma_0) \cdot (\gamma - \gamma_0)$$

$$+ V \int_{\gamma_0}^{\gamma} f(\gamma')\mathrm{d}\gamma' + \Delta E_{\mathrm{naf}}(\gamma),$$

where $\Delta\tau(x, \gamma_0) = \tau(x, \gamma_0) - \tau(x_{m,\gamma_0}, \gamma_0)$ and x_{m,γ_0} is the location of the starting minimum energy configuration along the MEP at γ_0. That is to say, the MEP for a given ST event under a macroscopic strain level γ can be estimated provided its MEP and the corresponding shear stress for each configuration along the MEP at a referential strain γ_0 are known. In turn, the locations of the minimum energy $(x_{m,\gamma})$ and the saddle point $(x_{s,\gamma})$ configurations, as well as the activation energy $(Q(\gamma) = E(x_{s,\gamma}, \gamma) - E(x_{m,\gamma}, \gamma))$ can also be easily deduced.

A closer inspection of Eq. 5 reveals that the last three terms do not contribute to the activation energy, instead, they merely set a baseline for the MEP at the macroscopic strain level of γ with respect to that of γ_0 and can therefore be ignored if only the activation energy is of interest.

III. METHODS

Since it is neither practical to examine the energy landscape of a metallic glass experimentally, nor is it feasible to track the variation of the MEP pertinent to an ST event, atomistic scale modeling is employed to confirm the above analysis. The $Cu_{64}Zr_{36}$ metallic glass is chosen as our model system, which has a high glass forming ability and has been extensively studied in the literature [25–29]. The interatomic interactions are described by an Embedded Atom Method (EAM) potential parameterized by Cheng *et al.* [30], which has been successfully employed to investigate various structural and energetic properties of the Cu-Zr system [21, 28, 29, 31]. The metallic glass model was prepared by beginning with a cubic simulation box containing $10,000$ atoms, equilibrated at $2,500$ K (which is much higher than the equilibrium liquidus temperature of $Cu_{64}Zr_{36}$) for 10 ns to ensure chemical and structural homogeneity. The melt was then quenched to room temperature (300 K) at a cooling rate of 10^9 K/s using a Nose-Hoover thermostat and barostat to monitor the

temperature and pressure (maintained at ~ 1 bar), respectively. The glass model was then relaxed to its local energy minimum using the conjugate gradient method, during which the box size was allowed to adjust so as to maintain a pressure around zero.

To harvest the local energy landscape of ST events in a deformation process, athermal quasi-static shear (AQS) [32] was applied to the obtained glass model until a macroscopic shear strain of 0.15 at a step-size of 1×10^{-5}, during which the Fast Inertial Relaxation Engine (FIRE) [33] was turned on to minimize the total energy of the system. It can be expected that when the strain is large enough, ST events will be triggered in the system. The selection of the ST event for detailed study is however non-trivial: one should isolate the event from others that might occur in other regions of the metallic glass, so as to avoid the interference of the ST event under study. Here we choose the first three shear transformation events identified from the stress-strain curve as examples for detailed analysis. The von-Mises atomic shear strain [34] was employed to confirm the occurrence of an ST event, by detecting when a peak value of the von-Mises atomic shear strain is observed for a cluster of atoms. This also corresponds to a stress drop in the stress-strain curve. The following procedures were then followed to evaluate the MEPs of each ST event at different macroscopic shear strains, as illustrated in Fig. 1: First, the atomic configuration right after the ST was chosen as a starting point to unload the system, reversing the shear applied to the system, until the reverse ST occurred. The unloading prior to the reverse ST generates shear transformed atomic configurations at different macroscopic strain levels. Secondly, configurations from the loading and the unloading curves corresponding to a same macroscopic strain were used as the initial and final configurations for subsequent nudged elastic band (NEB) calculations, so as to measure the MEP of the associated ST at a given macroscopic strain level. The NEB calculations were performed with a force tolerance of 5×10^{-4} eV/Å using 32 images, and cubic spline interpolations were employed to estimate the necessary information for unmeasured configurations along the MEP.

IV. RESULTS AND DISCUSSIONS

The initial part of the (shear) stress-strain curve from the AQS process shown in Fig. 2 behaves roughly linearly. A closer examination however reveals many sudden stress drops even in the "linear" region, suggesting the occurrences of ST events. The first three were
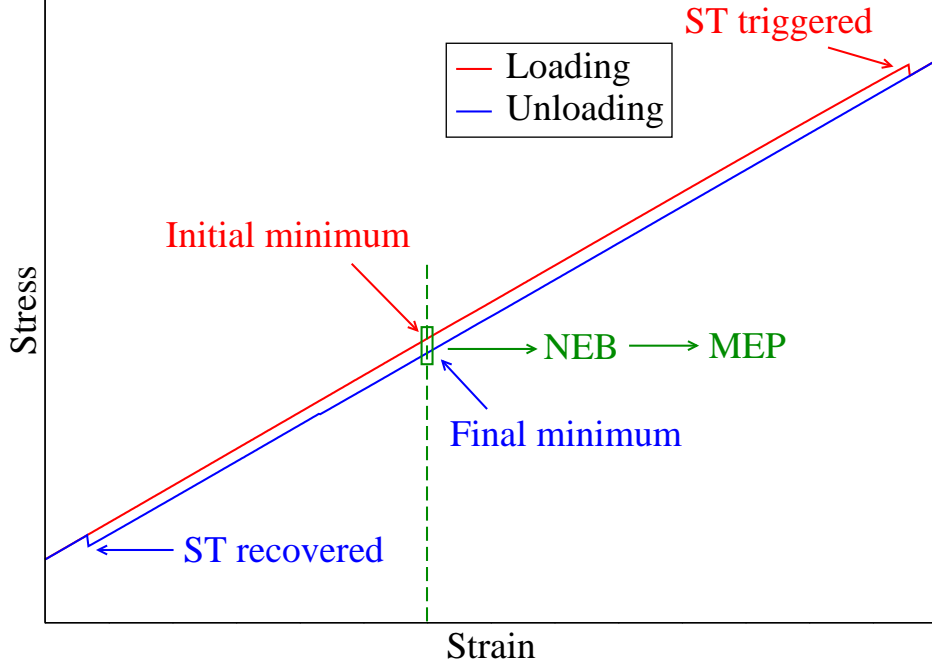
6

FIG. 1. Illustration of the procedure adopted to evaluate the MEP at different macroscopic strains for an ST event. Firstly, the triggering point of the ST event is identified, and then the recovering point along the loading and unloading curves, respectively. Secondly, for a given macroscopic strain in between of these two points, take the configuration on the loading curve and that on the unloading curve as the initial and final configurations for subsequent NEB calculations to measure the MEP at this strain level and in turn the activation energy.

observed at macroscopic shear strains of 0.0098, 0.0178, and 0.0248, respectively. We will take the ST event triggered at $\gamma = 0.0248$ as our first example to examine the strain dependence of its activation energy. Unloading of the transformed configuration revealed that a negative stress is needed to recover this transformation. In order to avoid interference with the other ST events (those that took place at 0.0098 and 0.0178, respectively), the NEB calculations were performed at macroscopic strains of 0.0010, 0.0100, 0.0130, 0.0200, and 0.0230. Fig. 3(a) shows the MEPs and Fig. 3(b) shows the relative stresses obtained, where the reaction coordinate x is given by the distance to the initial minimum configuration at $\gamma_0 = 0.0010$. It should be noted that for all the MEPs, the energy of the starting configuration was shifted to zero, and the relative stresses are given by $\Delta\tau(x, \gamma) = \tau(x, \gamma) - \tau(x_{m,\gamma}, \gamma)$. One sees that in general, an energy barrier is present in each MEP and the MEP is asymmetric. The asymmetry is enhanced upon further deformation: the barrier
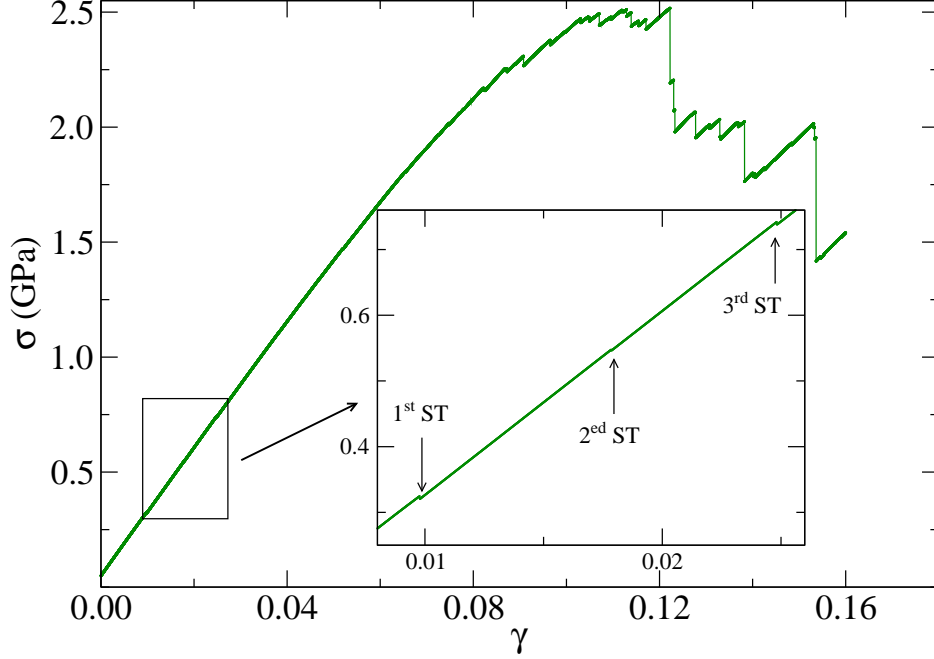
FIG. 2. Stress-strain curve of the athermal quasi-static shear process. The inset reveals the stress drops corresponding to the triggering of the first three STs.

for forward transformation decreases with the increasing of the macroscopic strain, while that for the backward transformation increases. This was further manifested in Fig. 4(a): one sees that the forward barrier approaches zero when the macroscopic strain approaches 0.0248, where the ST event occurs. One also sees from Fig. 3 and Fig. 4(b) that the location of the starting minimum energy configuration and that of the saddle point configuration vary with the macroscopic strain levels. With the increasing of γ, $x_{m,\gamma}$ shows a right shift, i.e., shifts towards the saddle point configuration. Conversely, $x_{s,\gamma}$ shifts left, towards $x_{m,\gamma}$. They meet with each other when the ST event occurs spontaneously, corresponding to the strain level with a zero barrier for the event.

Accompanying the MEP calculation, the stress for each image along the MEP was also obtained. One sees from Fig. 3(b) that the stress difference $\Delta\tau(x,\gamma)$ shows a linear decrease with increasing the reaction coordinate x. This is however counter-intuitive, as when the barrier is crossed, one would expect some variations in the stress as well, such as a sinusoidal variation suggested by Schuh *et al.* [35]. Upon further consideration, this is quite understandable, as the ST event happens locally and affects only a small portion of the system. If one divides the system into an ST region and a matrix–consisting of the remaining material,
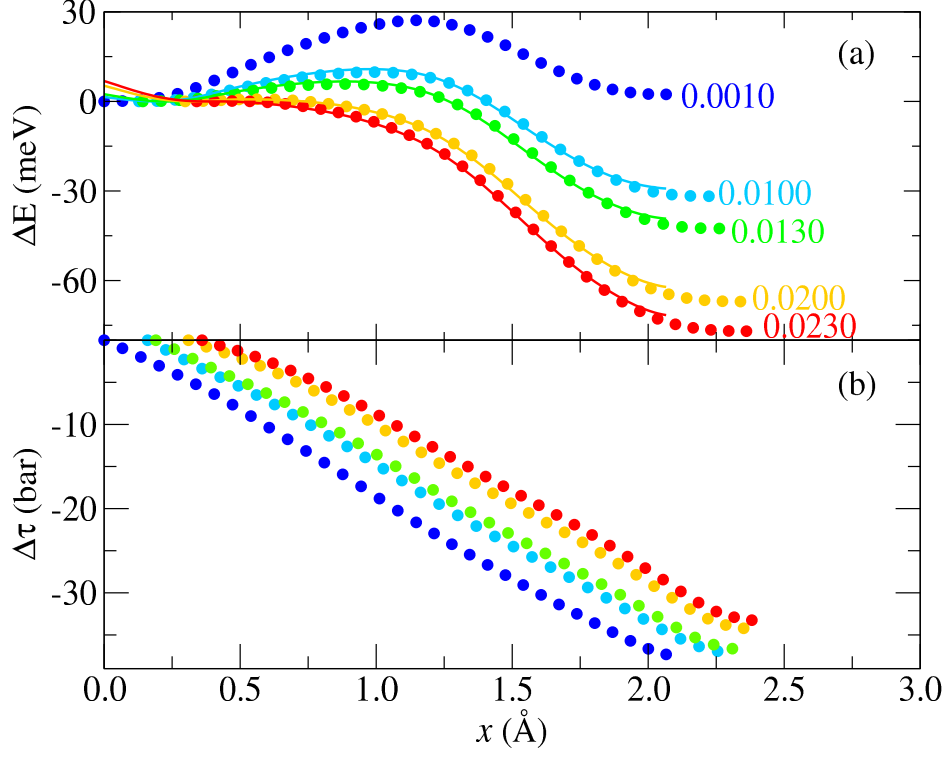
8

FIG. 3. (a) MEPs of the third ST event identified under different macroscopic strain levels from NEB calculations (circles) and estimations starting from the one measured at $\gamma_0 = 0.0010$ (lines). (b) Stress difference $(\Delta\tau(x,\gamma) = \tau(x,\gamma) - \tau(x_{m,\gamma},\gamma))$ from the NEB calculations.

similar variations can be observed in the "local" stress of the ST region, as evidenced in Fig. 5(b). Here the ST region was identified as a spherical region with relatively large atomic von-Mises strains, of a radius of ~ 5.2 Å. Since the occurrence of the ST event would "relax" the system, the stress in the matrix is partially relieved, the large volume share of the matrix thus dominates the stress variation, a monotonic decrease in $\Delta\tau(x,\gamma)$ with increasing the reaction coordinate is consequently observed.

Nevertheless, with the information on both the MEP and the stress variation in hand, the MEP at various strain levels can be deduced numerically according to Eq. 5. We therefore begin with the MEP and the stress difference along the MEP measured at $\gamma_0 = 0.0010$, and deduce the MEPs at $\gamma = 0.0100, 0.0130, 0.0200$, and 0.0230, shown in Fig. 3(a) as lines. One sees that the agreement with the NEB measurements is reasonably good, suggesting that the theory derived is promising in estimating the strain dependence of the MEP and the activation energy.
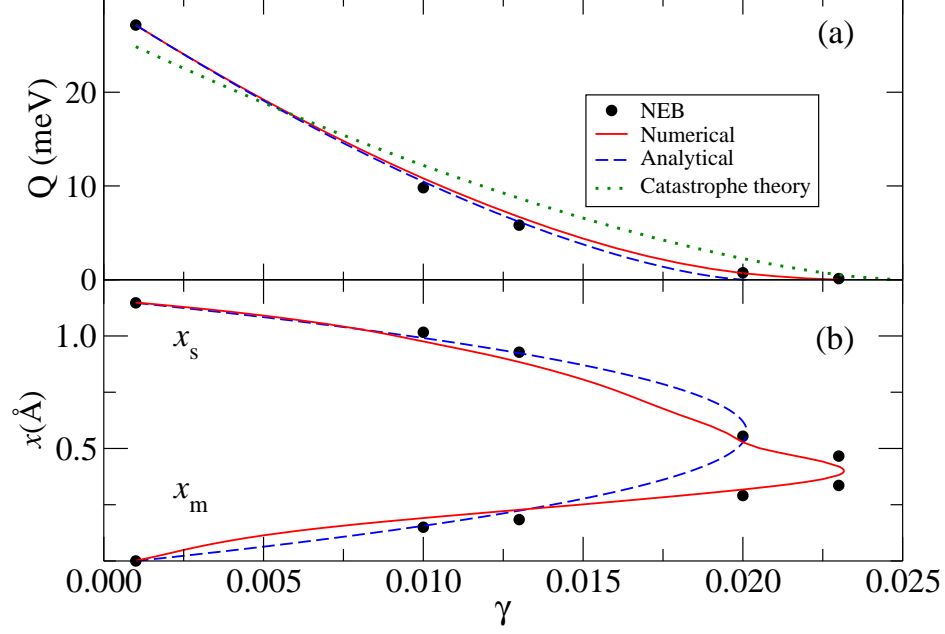
FIG. 4. (a) Activation energies of the third ST event at different stain levels as given by NEB calculations (black circle), numerical estimations (red solid line), analytical predictions (blue dashed line), and catastrophe theory fitting (green dotted line, fitting NEB results with $Q(\gamma) = k_Q(0.0248 - \gamma)^{\frac{3}{2}}$. 0.0248 is the triggering strain, where a stress drop occurs in AQS.). (b) The locations of the minimum energy configuration and the saddle point configuration along the MEP of the third ST event under different macroscopic strain levels. The red solid line is derived by minimizing/maximizing Eq. 5 numerically based on NEB calculations at $\gamma_0 = 0.0010$, and the blue dashed line is deduced according to Eq. 15 by taking $\gamma_0 = 0.0010$ as the reference.

An analytical expression will be of great help to understand the variations of the MEP, as in the catastrophe theory [14]. In this regard, the linear dependence of $\tau(x, \gamma_0)$ on x as seen in Fig. 3(b) can be approximated by

$$\tau(x, \gamma_0) = kx + \tau_{x_m,\gamma_0,\gamma_0}, \tag{6}$$

setting $x_{m,\gamma_0} = 0$, where $k = \frac{\tau_{x_s,\gamma_0} - \tau_{x_m,\gamma_0}}{x_{s,\gamma_0}}$, with τ_{x_s,γ_0} and τ_{x_m,γ_0} are the stresses of the saddle point configuration and the initial minimum energy configuration along the MEP of γ_0,
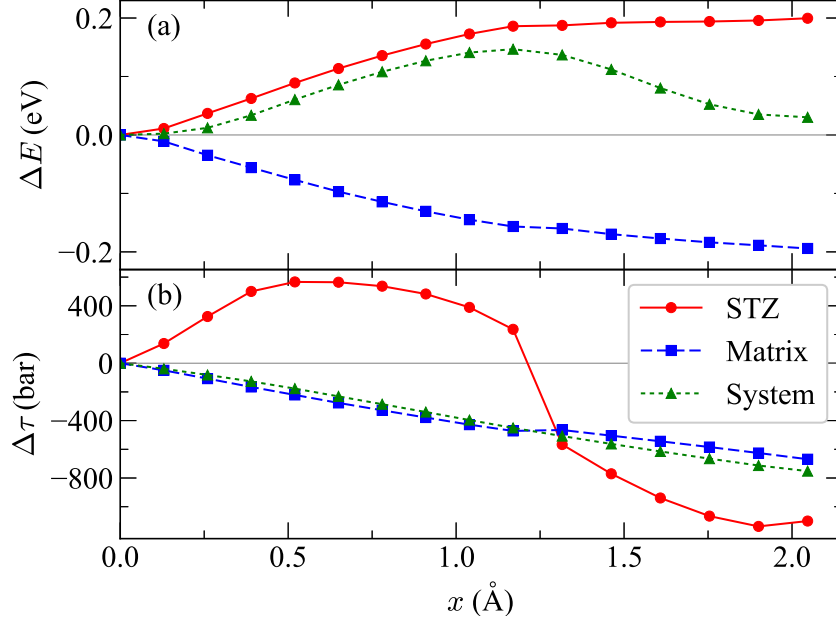
FIG. 5. (a) The variations in relative energies ($\Delta E(x) = E(x, \gamma_0) - E(x_{m,\gamma_0}, \gamma_0)$) and (b) relative stresses ($\Delta\tau(x) = \tau(x, \gamma_0) - \tau(x_{m,\gamma_0}, \gamma_0)$) as a function of reaction coordinate for the ST region (red circle), the remaining matrix (blue square), and the whole system (green triangle) for the third ST event at $\gamma_0 = 0.0010$. For clarity, the relative energy of the whole system (green triangle) in (a) is enlarged by a factor of 5, and the relative stresses for both the matrix (blue square) and the whole system (green triangle) in (b) are amplified by 20 times.

respectively. With Eq. 6, Eq. 5 can be simplified as

$$
\begin{aligned}
E(x, \gamma) &= E(x, \gamma_0) + V \cdot kx \cdot (\gamma - \gamma_0) + V \cdot \tau_{x_{m,\gamma_0}, \gamma_0}(\gamma - \gamma_0) \qquad (7)\\
&\quad + V \int_{\gamma_0}^{\gamma} f(\gamma')\mathrm{d}\gamma' + \Delta E_{\mathrm{naf}}(\gamma),\\
&= E(x, \gamma_0) + Vkx \cdot (\gamma - \gamma_0) + E'(\gamma),
\end{aligned}
$$

where $E'(\gamma) = V \cdot \tau_{x_{m,\gamma_0}, \gamma_0}(\gamma - \gamma_0) + V \int_{\gamma_0}^{\gamma} f(\gamma')\mathrm{d}\gamma' + \Delta E_{\mathrm{naf}}(\gamma)$ is the contribution to $E(x, \gamma)$ that depends only on γ. This formula is quite similar to the one used to describe the MEP variation in the catastrophe theory [14], which approximates the MEP by a third or forth order Taylor expansion around the critical point. It should be pointed out that all the terms in Eq. 7 can be extracted from the atomistic model, and no fitting to other properties is needed. The similarity between these two formulae suggests that the law
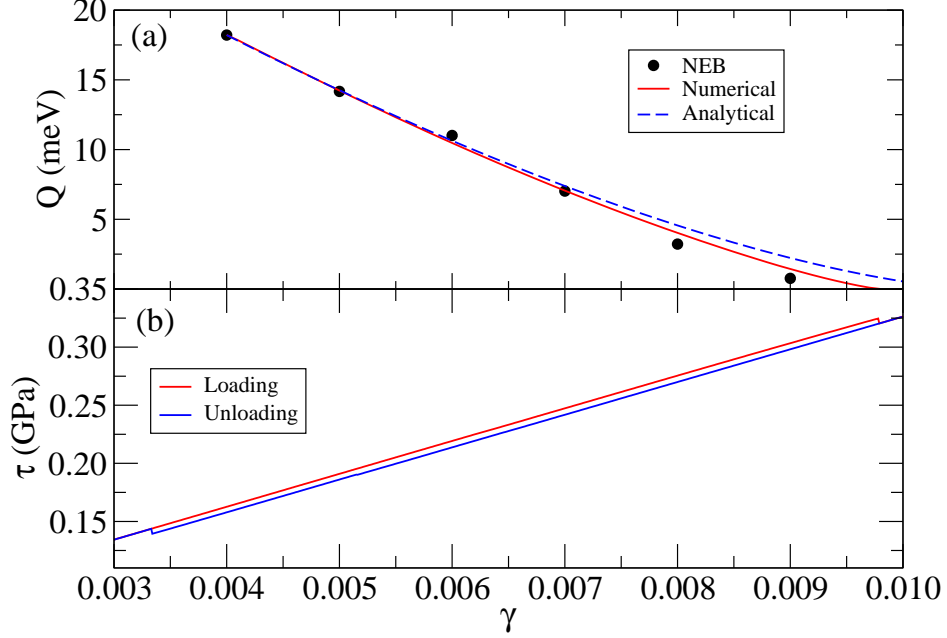
11

FIG. 6. (a) Activation energies of the ST event triggered at 0.0098 at different strain levels from NEB calculations (hollow point), numerical estimations (red solid line), and analytical predictions (blue dashed line). (b) Macroscopic shear stress-strain curves during loading (red) and unloading (blue) for the first identified ST event. The event was reversed at a strain of 0.0033.

derived in the catastrophe theory is valid only when the stress varies linearly (Eq. 6). It is however noticed that the linearity assumption does not always hold. For example, for the third ST event another component σ_{xz} ($\tau = \sigma_{xy}$ in Fig. 3(b)) along MEP did not follow the linearity assumption. Thus, it may be unreliable to predict the activation energy under shear deformation along XZ direction with the analytical formula (Eq. 7). In the appendix, we will show an example where a linear variation of the shear stress as a function of the reaction coordinate is not followed, leading to an incorrect prediction of the activation energy for such event. Nonetheless, even under such conditions, the present model based on Eq. 5 still works in a wide strain range up to strain 0.08, except that the simplification of Eq. 7 does not hold any more. Consequently, care should be taken when one relies on the assumed linearity in applying the catastrophe theory or our analytical formula (Eq. 7), especially for regions far away from the referential critical point.
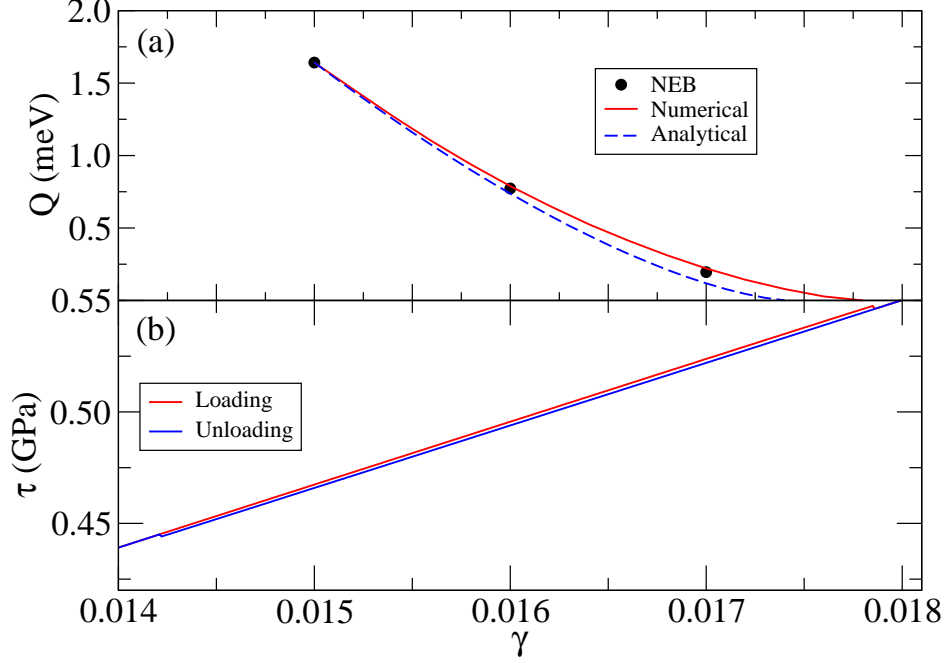
FIG. 7. (a) Activation energies of the ST event triggered at 0.0178 at different strain levels from NEB calculations (hollow point), numerical estimations (red solid line), and analytical predictions (blue dashed line). (b) Macroscopic shear stress-strain curves during loading (red) and unloading (blue) for the second identified ST event. The event was reversed at a strain of 0.0143.

Noticing that the first half of the MEP satisfies three conditions (setting $x_{m,\gamma_0} = 0$):

$$\left.\frac{\partial E(x, \gamma_0)}{\partial x}\right|_{x=0} = 0, \tag{8}$$

$$\left.\frac{\partial E(x, \gamma_0)}{\partial x}\right|_{x=x_s} = 0,$$

$$E(x_s, \gamma_0) - E(0, \gamma_0) = Q_{\gamma_0},$$

it can therefore be approximated by a cubic polynomial

$$E(x, \gamma_0) = Ax^3 + Bx^2 + Cx + E(0, \gamma_0), \tag{9}$$

and can be solved as

$$E(\tilde{x}, \gamma_0) = -2Q_{\gamma_0}\tilde{x}^3 + 3Q_{\gamma_0}\tilde{x}^2 + E(0, \gamma_0), \tag{10}$$

where a scaled reaction coordinate is defined as $\tilde{x} = x/x_{s,\gamma_0}$. Inserting Eq. 10 into Eq. 7, we arrive at an analytical expression for the MEP at γ

$$E(\tilde{x}, \gamma) = -2Q_{\gamma_0}\tilde{x}^3 + 3Q_{\gamma_0}\tilde{x}^2 + V\tilde{x} \cdot \Delta\tau_0 \cdot (\gamma - \gamma_0) + E'(\gamma), \tag{11}$$

13

where $\Delta \tau_0 = \tau_{\tilde{x}_s, \gamma_0, \gamma_0} - \tau_{0, \gamma_0}$ is the stress difference between the saddle point configuration and the initial equilibrium configuration at γ_0. By locating the first minimum and maximum of $E(\tilde{x}, \gamma)$ with respect to $\tilde{x}$, one obtains the locations of the starting minimum configuration and the saddle point configuration along the MEP at the macroscopic strain of γ. And they are found to be

$$\tilde{x}_s = \frac{3Q_{\gamma_0} + \sqrt{9Q_{\gamma_0}^2 + 6Q_{\gamma_0} V \Delta \tau_0 \Delta \gamma}}{6Q_{\gamma_0}}, \tag{12}$$
$$\tilde{x}_m = \frac{3Q_{\gamma_0} - \sqrt{9Q_{\gamma_0}^2 + 6Q_{\gamma_0} V \Delta \tau_0 \Delta \gamma}}{6Q_{\gamma_0}},$$

where $\Delta \gamma = \gamma - \gamma_0$. The analytic expression for the activation energy as a function of the macroscopic strain is accordingly given by

$$Q(\gamma) = Q_{\gamma_0} \left(1 + \frac{2V \Delta \tau_0 \Delta \gamma}{3Q_{\gamma_0}} \right)^{\frac{3}{2}}, \tag{13}$$

and activation energy vanishes at a triggering strain of

$$\Delta \gamma_c = -\frac{3Q_{\gamma_0}}{2V \Delta \tau_0}. \tag{14}$$

By employing Eq. 14, the critical strain for the third ST event is "predicted" to be 0.0201, while that estimated numerically based on Eq. 5 is 0.0231, both agree reasonably well with the AQS value of 0.0248. Comparatively, the numerical estimation has a better agreement with the AQS value than the analytical one, while the latter is more convenient to use/evaluate than the former. Inserting Eq. 14 into Eq. 13 and Eq. 12, we can obtain

$$Q(\gamma) = Q_{\gamma_0} \left(1 - \frac{\Delta \gamma}{\Delta \gamma_c} \right)^{\frac{3}{2}}, \tag{15}$$
$$\tilde{x}_s = \frac{1}{2} + \frac{1}{2}\sqrt{1 - \frac{\Delta \gamma}{\Delta \gamma_c}},$$
$$\tilde{x}_m = \frac{1}{2} - \frac{1}{2}\sqrt{1 - \frac{\Delta \gamma}{\Delta \gamma_c}}.$$

Besides an apparent strain dependence in the activation energy similar to the catastrophe theory [14], one sees from the above expressions that in order to predict the activation energy at a strain level of γ, it would be sufficient to know Q_{γ_0} and the stress difference between the saddle point configuration and the starting minimum energy configuration along the MEP at a referential strain level of γ_0. It is worth noting that a similar form of $\tilde{x}_m$ was

14

proposed by Maloney *et al.* [23] based on normal mode analysis. The activation energies for the third ST event under different strains were estimated according to the analytic expression of Eq. 15 and shown in Fig. 4(a) as dashed lines. In addition, the locations of the starting minimum energy configuration and the saddle point configuration were also deduced according to Eq. 15, which were compared in Fig. 4(b) to those derived by finding the minimum and maximum of Eq. 5 numerically and the NEB results. **Incidentally, one reads from Eq. 15 that Q scales to $(1 - \Delta\gamma/\Delta\gamma_c)^{3/2}$, while seperation between $\tilde{x}_s$ and $\tilde{x}_m$ scales to $(1 - \Delta\gamma/\Delta\gamma_c)^{1/2}$, the former will converge to zero much faster than the latter, in line with the observation in Fig. 4 where the activation energy diminishes while the seperation between $\tilde{x}_s$ and $\tilde{x}_m$ still seems to be large in the NEB calculations. Nonetheless, one sees from Fig. 4 that** the estimations agree reasonably well with the NEB results, suggesting that prediction based on the analytic approximation is feasible. Its advantage over the numerical approach is that one only needs the information of the minimum energy configuration and the saddle point configuration along the MEP at the referential strain level, instead of those along the entire MEP. The scaling law of $Q = k_Q(\gamma_c - \gamma)^{\frac{3}{2}}$ (here γ_c is the triggering strain at which Q vanishes in AQS) from the catastrophe theory [14] is also fitted as shown in Fig. 4(a) as a dotted line for comparison.

Beginning with Eq. 13, the shear activation volume, defined as negative of the first derivative of the activation energy with respect to the shear stress, can be given by

$$V^*(\gamma_0) = -V\Delta\tau_0 \frac{d\gamma}{d\tau}\bigg|_{\gamma=\gamma_0}, \tag{16}$$
$$= -\frac{V\Delta\tau_0}{G(\gamma_0)},$$
$$= \frac{3Q_{\gamma_0}}{2\Delta\gamma_c G(\gamma_0)},$$

$$V^*(\gamma) = -V\Delta\tau_0 \sqrt{\frac{3Q_{\gamma_0} + 2V\Delta\tau_0\Delta\gamma}{3Q_{\gamma_0}}} \frac{d\gamma}{d\tau}, \tag{17}$$
$$= \frac{3Q_{\gamma_0}}{2\Delta\gamma_c G(\gamma)} \sqrt{1 - \frac{\Delta\gamma}{\Delta\gamma_c}},$$

where $G(\gamma)$ is the athermal shear modulus of the whole system. And if $G(\gamma) \approx G(\gamma_0)$, then

$$V^*(\gamma) = V^*(\gamma_0) \sqrt{1 - \frac{\Delta\gamma}{\Delta\gamma_c}}. \tag{18}$$

15

Incidentally, the stress change of the system upon deformation from γ_0 to γ can also be expressed by

$$\tau(\tilde{x}_{m,\gamma}, \gamma) = \tau(0, \gamma) + \Delta\tau_0 \cdot \tilde{x}_{m,\gamma}, \tag{19}$$

$$= \tau(0, \gamma) + \Delta\tau_0 \left(\frac{1}{2} - \frac{1}{2}\sqrt{1 - \frac{\Delta\gamma}{\Delta\gamma_c}} \right).$$

Therefore, the athermal shear modulus of the system can be derived as

$$G(\gamma) = \frac{\mathrm{d}\tau(\tilde{x}_{m,\gamma}, \gamma)}{\mathrm{d}\gamma}, \tag{20}$$

$$= \frac{\mathrm{d}\tau(0, \gamma)}{\mathrm{d}\gamma} + \frac{\Delta\tau_0}{4\sqrt{\Delta\gamma_c(\Delta\gamma_c - \Delta\gamma)}},$$

$$= \frac{\mathrm{d}\tau(0, \gamma)}{\mathrm{d}\gamma} - \frac{1}{4\sqrt{\Delta\gamma_c(\Delta\gamma_c - \Delta\gamma)}} \cdot \frac{V^*(\gamma_0)}{V} \cdot G(\gamma_0),$$

where the second term is the nonlinear contribution to the modulus of the system from the ST event. Supposing that $G(\gamma_0)$ is close to $G(\gamma)$ and that $V^*(\gamma_0)$ is insensitive to the system size, when the system volume V is small and/or when the macroscopic strain approaches the critical strain, the nonlinear contribution of the event becomes prominent, and one can then predict the critical strain of the ST event by examining the modulus or stress variation against the macroscopic strain [36–38]. This also explains why the error in the predicted critical strain becomes large when the system volume increases [36].

All the discussions up to now have considered only the third ST event identified in the AQS process as an example, while the theoretical framework derived should work with any other ST event. To further confirm this, the activation energies, critical strains of the first and the second ST events identified under different macroscopic strain levels were also worked out following both the numerical and analytical recipes. One finds from Fig. 6 and Fig. 7 again that both approaches give reasonable agreement with the NEB calculations. The comparison of the critical strains shown in Table I also reveal very good agreement between the predictions and the simulations, confirming the reliability of the underlying theoretical model as well as the methods.

V. CONCLUSION

In summary, the stain dependence in the activation energies of local shear transformation events in metallic glasses were investigated both theoretically and computationally.

The theoretically analysis suggests not only a dependence on the macroscopic strain in the activation energies of local shear transformation events, but also that the dependence can be predicted based on the information at a referential strain level. Numerical calculations based on athermal quasi-static shear simulation and nudged elastic band calculations prove that the proposed theory works well, and also reveal that the dependence can be expressed analytically with reasonable approximations. The analytical approach is seen to yield comparable agreement to the exact NEB calculations as that of the numerical predictions. This opens the possibility of fast algorithms that are able to infer the character of statistically significant number of energy barriers in the glass and the evolution of their distributions during thermal and/or mechanical processing.

It is widely accepted that the potential energy landscape provides a very useful perspective to describe the mechanical behavior of metallic glasses. Due to its hyper-dimensional nature and complex coupling with the surrounding environment, it is unreasonable to expect that a complete characterization of the energy landscape is achievable or desirable. Rather atomistic modeling provides a methodology by which the specific aspects of the energy landscape that are crucial for determing important material properties are identified and characterized. The present approach, by effectively capturing the features of the potential energy landscape that are most closely associated with shear induced atomic-scale rearrangement, therefore provides a powerful tool to understand the mechanical deformation of metallic glasses, and perhaps also the mechanical behavior of disordered systems more generally.

TABLE I. Comparison of the triggering strains for the first three ST events determined by AQS, numerical estimation, and analytical prediction.

ST Event	AQS	Numerical	Analytical
1st	0.0098	0.0098	0.0106
2nd	0.0178	0.0178	0.0174
3rd	0.0248	0.0231	0.0201

ACKNOWLEDGMENTS

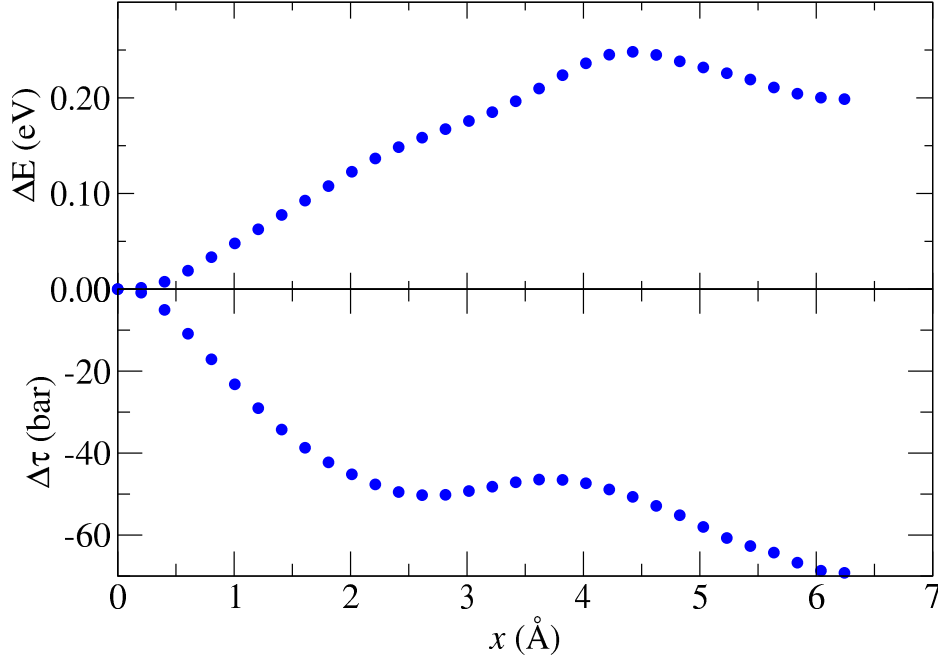## Appendix: An example not following stress linearity assumption

FIG. A1. Stress and energy information along the MEP.

In this appendix, we will illustrate an example where the shear stress does not vary linearly as a function of the reaction coordinate, resulting in failure of the activation energy prediction based on the analytical approach. The example was captured when we were trying to predict the triggering strains of all the ST events identified in the Cu-Zr metallic glass based on the Activation Relaxation Technique (ARTn) [39–41]. It turned out that the predictions based on Eq. 7 fail for some of the events, and further analysis revealed that for
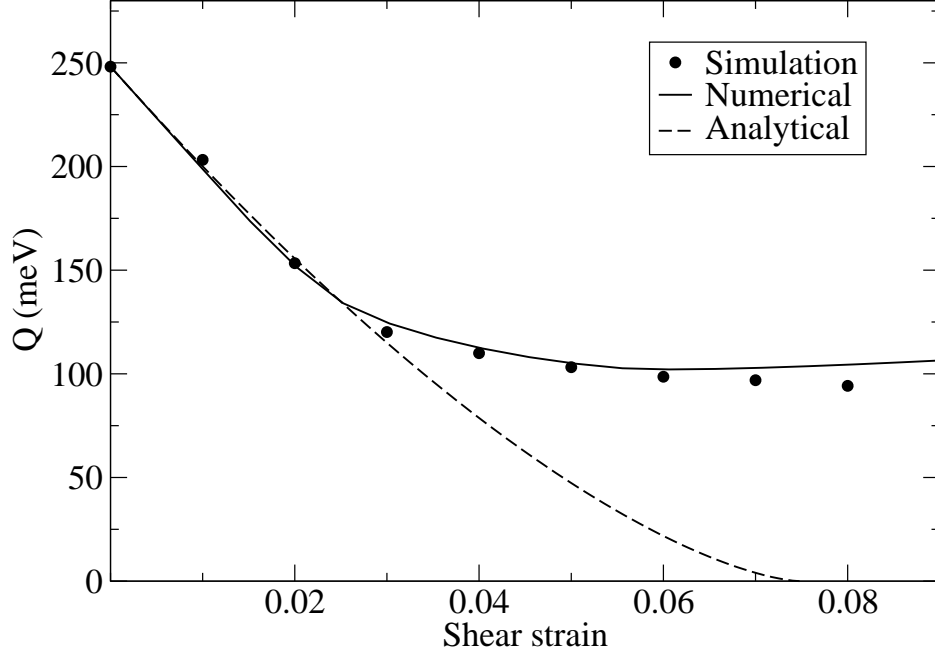
18

FIG. A2. Variation of activation energy against the macroscopic strain. Points, dashed line, solid line are results from the NEB calculation, the numerical estimation and the analytical prediction, respectively.

such events, the variation of the shear stress as a function of the reaction coordinate does not show a linear behavior, as is seen in Fig. A1. Nonetheless, numerical prediction based on Eq. 5 still yields reasonable agreement with the direct calculations. It is worth to note that since no triggering strain existed in this event, it is impractical to apply catastrophe theory to study the strain dependence of activation energy in such situation.

[1] W. Klement, R. H. Willens, and P. Duwez, Nature **187**, 869 (1960).

[2] F. Spaepen, Acta Metall. **25**, 407 (1977).

[3] A. Argon, Acta Metall. **27**, 47 (1979).

[4] V. V. Bulatov and A. Argon, Modell. Simul. Mater. Sci. Eng. **2**, 167 (1994).

[5] M. L. Falk and J. S. Langer, Phys. Rev. E **57**, 7192 (1998).

[6] W. L. Johnson and K. Samwer, Phys. Rev. Lett. **95**, 195501 (2005).

[7] M. D. Demetriou, J. S. Harmon, M. Tao, G. Duan, K. Samwer, and W. L. Johnson, Phys. Rev. Lett. **97**, 065502 (2006).

[8] J. S. Langer, Phys. Rev. E **77**, 021502 (2008).

[9] M. L. Falk and J. S. Langer, Annual Review of Condens. Matter Phys. , 28 (2010).

[10] H. Eyring, The J. Chem. Phys. **4**, 283 (1936).

[11] P. Zhao, J. Li, and Y. Wang, Acta Mater. **73**, 149 (2014).

[12] E. R. Homer and C. A. Schuh, Acta Mater. **57**, 2823 (2009).

[13] L. Li, E. R. Homer, and C. A. Schuh, Acta Mater. **61**, 3347 (2013).

[14] C. E. Maloney and D. J. Lacks, Phys. Rev. E **73**, 061106 (2006).

[15] S. M. Avdoshenko and D. E. Makarov, J. Chem. Phys. **142** (2015), 10.1063/1.4919541.

[16] T. Zhu, J. Li, A. Samanta, A. Leach, and K. Gall, Phys. Rev. Lett. **100**, 025502 (2008).

[17] J. P. K. Doye, M. A. Miller, and D. J. Wales, The J. Chem. Phys. **111**, 8417 (1999).

[18] H. Kallel, N. Mousseau, and F. Schiettekatte, Phys. Rev. Lett. **105**, 045503 (2010).

[19] T. F. Middleton and D. J. Wales, J. Chem. Phys. **118**, 4583 (2003).

[20] D. Rodney and C. Schuh, Phys. Rev. Lett. **102**, 235503 (2009).

[21] Y. Fan, T. Iwashita, and T. Egami, Nat. Commun. **5**, 5083 (2014).

[22] P. Cao, X. Lin, and H. S. Park, J. Mech. Phys. Solids **68**, 239 (2014).

[23] C. Maloney and A. Lemaître, Phys. Rev. Lett. **93**, 195501 (2004).

[24] Y. Q. Cheng and E. Ma, Phys. Rev. B **80**, 064104 (2009).

[25] D. Xu, B. Lohwongwatana, G. Duan, W. L. Johnson, and C. Garland, Acta Mater. **52**, 2621 (2004).

[26] A. J. Cao, Y. Q. Cheng, and E. Ma, Acta Mater. **57**, 5146 (2009).

[27] H. Tian, C. Zhang, L. Wang, J. Zhao, C. Dong, B. Wen, and Q. Wang, J. Appl. Phys. **109**, 123520 (2011).

[28] J. Ding, S. Patinet, M. L. Falk, Y. Cheng, and E. Ma, Proc. Natl. Acad. Sci. U.S.A. **111**, 14052 (2014).

[29] J. Ding, Y. Q. Cheng, and E. Ma, Acta Mater. **69**, 343 (2014).

[30] Y. Q. Cheng, E. Ma, and H. W. Sheng, Phys. Rev. Lett. **102**, 245501 (2009).

[31] Y. Q. Cheng, H. W. Sheng, and E. Ma, Phys. Rev. B **78**, 014207 (2008).

[32] C. E. Maloney and A. Lemaître, Phys. Rev. E **74**, 016118 (2006).

[33] E. Bitzek, P. Koskinen, F. Gähler, M. Moseler, and P. Gumbsch, Phys. Rev. Lett. **97**, 170201 (2006).

[34] F. Shimizu, S. Ogata, and J. Li, Mater. Trans. **48**, 2923 (2007).

20

[35] C. a. Schuh and A. C. Lund, Nat. Mater. **2**, 449 (2003).

[36] S. Karmakar, A. Lemaître, E. Lerner, and I. Procaccia, Phys. Rev. Lett. **104**, 215502 (2010), arXiv:1002.3487.

[37] S. Karmakar, E. Lerner, and I. Procaccia, Phys. Rev. E **82**, 026105 (2010).

[38] R. Dasgupta, S. Karmakar, and I. Procaccia, Phys. Rev. Lett. **108**, 075701 (2012).

[39] N. Mousseau, L. K. Béland, P. Brommer, J.-F. J.-F. Joly, F. El-Mellouhi, E. Machado-Charry, M.-C. Marinica, and P. Pochet, Journal of Atomic, Molecular, and Optical Physics **2012**, 1 (2012).

[40] E. Cancès, F. Legoll, M. Marinica, K. Minoukadeh, and F. Willaime, The J. Chem. Phys. **130**, 114711 (2009).

[41] N. Mousseau and G. T. Barkema, Phys. Rev. E **57**, 2419 (1998).